Available online at www.sciencedirect.com

SciVerse ScienceDirect

Ceramics International 39 (2013) 51–56

CERAMICS INTERNATIONAL

www.elsevier.com/locate/ceramint

Influence of VO_2 nanostructured ceramics on hydrogen desorption properties from magnesium hydride

Sanja Milošević[a], Željka Rašković-Lovre[a], Sandra Kurko[a], Radojka Vujasin[a], Nikola Cvjetićanin[b], Ljiljana Matović[a], Jasmina Grbović Novaković[a,*]

[a]Department of Materials Science, Vinča Institute of Nuclear Sciences, University of Belgrade, P.O. Box 522, Belgrade 11 000, Serbia
[b]Faculty of Physical Chemistry, University of Belgrade, Studentski trg 12-16, Belgrade 11 000, Serbia

Received 10 April 2012; received in revised form 28 May 2012; accepted 29 May 2012
Available online 8 June 2012

Abstract

The hydrogen desorption properties and kinetics of MgH_2–VO_2 composite prepared by mechanical milling of MgH_2 and VO_2 have been investigated. Structural characterization of produced nanocomposite was done by X-ray powder diffraction (XRD), particle size analysis and scanning electron microscopy (SEM). The structure and morphology of the composite have been correlated with hydrogen desorption properties investigated by differential thermal analysis (DTA). It has been shown that short mechanical milling of nanostructured VO_2 and MgH_2 leads to decrease of hydrogen desorption temperature of MgH_2 by 80 K. The mechanism of desorption has been changed from phase boundary reaction, spherical symmetry for untreated MgH_2 to phase boundary reaction, cylindrical symmetry for the composite material. The activation energy for desorption has been reduced by adding VO_2 ceramics as a catalyst.

Keywords: A. Milling; Composites MgH_2–VO_2; Desorption; Non-isothermal kinetics

1. Introduction

Using hydrogen as an energy media via fuel cells represents one of the most promising ways to obtain sustainable energy. However, hydrogen is still not widely used as fuel, since the problem of its storage still exists. Having a media that can fulfill the requirements for mobile and stationary application would solve the hydrogen storage problem, but such material does not exist yet. For instance, even if some materials are very promising in the terms of hydrogen weight percents, their kinetics and cyclability performances are usually unsatisfactory. The best compromise between all desirable parameters is currently given by metal hydrides. The biggest attention among them is dedicated to magnesium hydride since its high hydrogen capacity by weight (7.6 wt%) and volume (102 g/L), low cost and high abundance of Mg [1]. Even though, MgH_2 possesses a rationally high gravimetric and volumetric capacity, the high temperature of decomposition and the poor absorption/desorption kinetics hinder its practical application. Much effort has been made to improve magnesium hydride performances and to overcome thermodynamic constraints ranging from alloying magnesium hydride with other elements or mixing it with catalysts to reduction of crystallite and particle size [2–9]. It was reported that the sorption kinetics of MgH_2 can be dramatically increased by ball milling with transition metals [9,10], metal oxides [11–16], fluorides [17] and metal halide as additives or catalysts [18]. It was also demonstrated that oxide additives are superior catalysts for hydrogen sorption although they exhibit a much lower dissociation probability for H_2 than 3d metals [7,19,20]. Oelerich et al. [12] compared the effects of different vanadium based additives (V_2O_5, metallic V, VN and VC) on the kinetics of hydrogen absorption–desorption in Mg/MgH_2 based systems. They have illustrated that

*Corresponding author. Tel.: +381 11 3408 552; fax: +381 11 3408 224.
E-mail address: jasnag@vinca.rs (J. Grbović Novaković).

0272-8842/$36.00
http://dx.doi.org/10.1016/j.ceramint.2012.05.091

V_2O_5 has beneficial effect on the desorption kinetics showing that the high valence state of TM metals plays also an important role in sorption kinetics. So far, the fastest rate for desorption of MgH_2 is achieved by small addition of Nb_2O_5 [3], but with extensive and long milling.

To improve desorption properties of MgH_2, VO_2(B) oxide phase is used as catalyst in this work. The structure of polymorph VO_2(B) is based on an oxygen bcc lattice with vanadium in the octahedral sites. The oxygen octahedra are slightly deformed and all vanadium atoms have a valency 4. The bcc oxygen sublattice in VO_2(B) has one vacancy per eight occupied sites. Milling such oxygen deficient oxide structure with MgH_2, will increase the number of defects and decrease the particle size which is expected to have a beneficial effect on the hydrogen desorption temperature of hydride.

2. Experimental part

MgH_2–VO_2 composites were prepared by ball milling of the commercial MgH_2 powder (Alfa Aeser, 98%) with 10 wt% of nanostructured VO_2 produced by one-step hydrothermal synthesis. The details of the VO_2 synthesis and structural characterization have been explained in previous work [21]. Milling process was performed under argon atmosphere for 10 h in Turbula Type 2TC Mixer using hardened steel vial and balls with ball to powder mass ratio fixed at 10:1. Since the peak broadening in XRD pattern is due to a combination of grain refinement (nanograin/crystallite) and the lattice strain effects, the separation of these two contributions was obtained from Cauchy/Gaussian approximation by the linear regression plot according to the following equation:

$$\frac{\delta^2(2\theta)}{\tan^2\theta} = \frac{k\lambda}{L}\left(\frac{\delta(2\theta)}{\tan\theta\sin\theta}\right) + 16e^2 \quad (1)$$

where the term $k\lambda/L$ is the slope, the parameter L is the mean dimension of the crystallites composing the powder particle, k is constant ($\sim$1) and e is the so-called "maximum" microstrain (calculated from the intercept), λ is the wave length and θ is the position of the analyzed peak maximum. Malvern 2000SM Mastersizer laser scattering particle size analysis system was used to obtain the quantitative MgH_2 particle size distribution. The specified resolution range of the system was sub-μm to 2 mm. 2-propanol was used as suspension media. All samples were ultrasonicated for 15 min prior to measurements. All measurements were performed in the same stirring speed and obscuration level. Morphological and microanalytical characterization was carried out by VEGA TS 5130 MM Tescan Brno SEM equipped with EDS detector while desorption properties of composites were followed by DTA measurements by SDT 2960 Instruments at a constant heating rate of 15 K/min, starting from room temperature to 830 K.

2.1. Mathematical treatment of thermal data

According to Sestak and Berggren [22], deduction of the mechanism of thermal decomposition process from non-isothermal (NI) data is based on the assumption that the NI reactions proceeds isothermally at an infinitesimal time interval, so that the reaction rate, $d\theta/dt$, can be expressed by Arrhenius type equation.

$$\frac{d\theta}{dt} = Ae^{\frac{-E^s_{des}}{RT}}f(\theta) \quad (2)$$

where A is the pre-exponential factor and $f(\theta)$ depends on the mechanism of the process involved. Further, for a linear heating rate β, $\beta = dT/dt$ and substitution into Eq. (2) gives:

$$\frac{d\theta}{f(\theta)} = \frac{A}{\beta}e^{\frac{-E^s_{des}}{RT}}dT \quad (3)$$

A large number of kinetic methods have been developed which are based on different forms of $f(\theta)$ (see Table 1). To evaluate the kinetic parameters from the previous equations, one can plot:

$$\ln\left[\frac{g(\theta)}{T^2}\right] = f\left(\frac{1000}{T}\right) \quad (4)$$

E^a_{des} and A can be calculated from the slope and intercept, respectively. The mechanism can be therefore obtained by searching for the best fit of the experimental data.

3. Results and discussion

Commercial sample (AA) shows narrow peaks typical for β-MgH_2 tetragonal structure and minor peaks corresponding to metallic Mg [6] (see Fig.1). XRD analysis of milled sample (V) shows additional peaks corresponding to VO_2(B) at $2\theta = 25.25$ and $Mg(OH)_2$ at $2\theta = 18.44$ and 38.10 although the samples were stored in inert atmosphere. Formation of $Mg(OH)_2$ could be a consequence of the fact that in the starting material traces of Mg has been found. During mechanical milling, Mg could react with residual moisture in the vial to form $Mg(OH)_2$. Broadening of typical β-MgH_2 peaks is directly used to determine the value of crystallite size of samples. It was found that the crystallite size of β-MgH_2 has been decreased during milling from 83 nm for untreated sample to 56 nm for milled one. This is well known fact which can be ascribed

Table 1
Commonly used $g(\theta)$ form for solid state reactions.

$g(\theta)$	Rate controlling process
$-\ln(1-\theta)$	Random nucleation one nucleus on each particle (Mampel equation-first order).
$1-(1-\theta)^{1\backslash 2}$	Phase boundary reaction, cylindrical symmetry
$1-(1-\theta)^{1\backslash 3}$	Phase boundary reaction, spherical symmetry
$-\ln(1-\theta)^{1\backslash 2}$	Random nucleation (Avrami equation I)
$-\ln(1-\theta)^{1\backslash 3}$	Random nucleation (Avrami equation I)

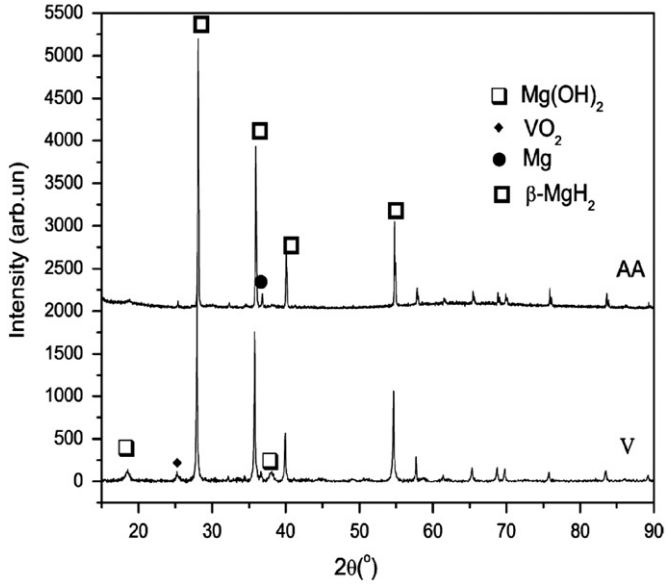

Fig. 1. XRD analysis of commercial MgH_2 powder (AA) and MgH_2–VO_2(B) composite (V).

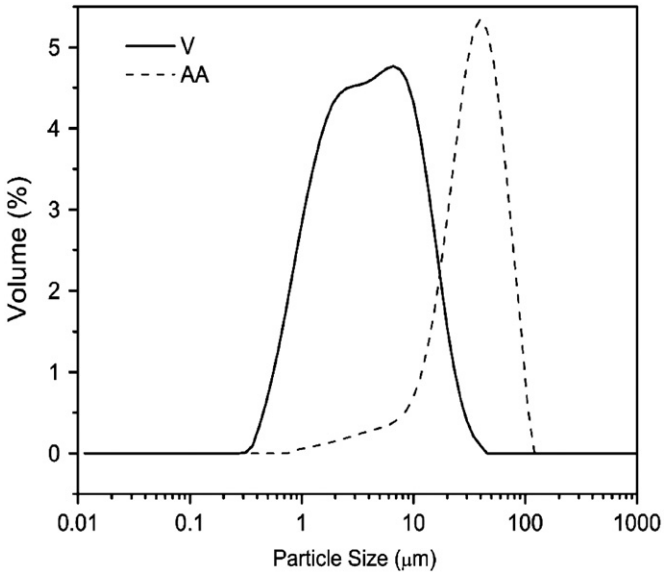

Fig. 2. Particle size distribution curves of a commercial MgH_2 powder (dashed line) and. MgH_2–VO_2(B) composite (solid line).

to the creation of dislocations [5]. Since the measured positions of MgH_2 peaks are slightly shifted from database positions this means that the lattice plane distances are changed, leading to expansion of MgH_2 unit cell and thus increasing the possibility of non-stoichiometric MgH_2 phase formation [19,23]. The particle size distribution curves for commercial MgH_2 and MgH_2 mechanically milled with VO_2(B), obtained by the laser scattering measurements are given in Fig. 2. The particles of commercial powder exhibit quite narrow monomodal distribution with mean particle size of 38 μm [24]. Ball milled sample reveals slight bimodal particle size distribution. 50% of particles show the average particle size around 2–3 μm, while another 50% has the size around 10 μm. Such distribution has an important influence on desorption properties of MgH_2 that leads to significant decrease of temperature (see DTA analysis). SEM micrographs of composites are shown in Fig. 3a and b. The MgH_2–VO_2(B) composite shows the presence of agglomerates with sizes ranging from 10 μm to 200 μm with quite different morphology. Smaller agglomerates exhibit the sponge-like structure (Fig. 3a) while the larger agglomerates have block-like structure, but with pronounced porous morphology (Fig. 3b).

The DTA spectra of commercial MgH_2 (AA) and mechanical milled sample with VO_2 (V) are given in Fig. 4. The pure MgH_2 sample has large desorption peak at 720 K (T^d_{max}) and small peak at 610 K, while catalyzed system shows three desorption maxima positioned at 642 K (high-temperature HT), 456 K (intermediate temperature-IT) and 354 K (low-temperature LT). The low temperature peaks (LT and IT) originate from H release from interface of MgH_2/$Mg(OH)_2$ as it was reported by Leardini et al. [25]. The existence of three desorption maxima indicates that induced defects create catalytically active sites, and in such way make possible the

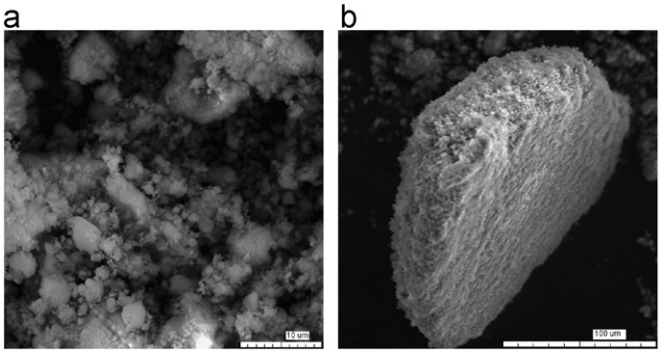

Fig. 3. SEM micrographs of MgH_2–VO_2(B) composite: (a) smaller agglomerates exhibit the sponge like structure; (b) larger agglomerates have block like structure but with pronounced porous morphology.

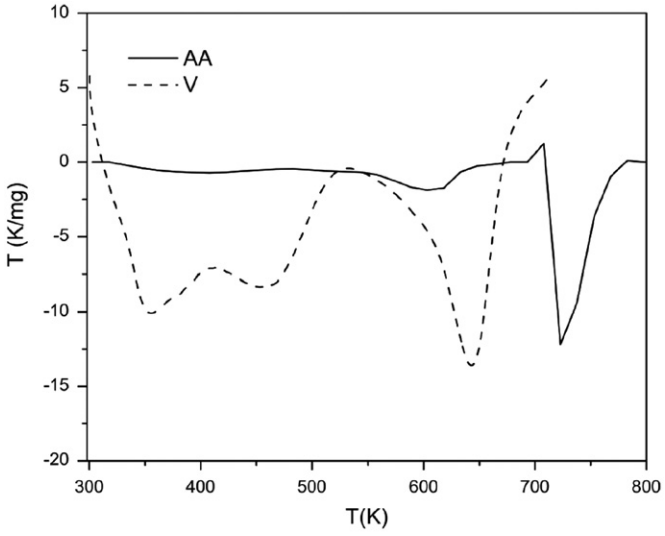

Fig. 4. DTA curves of a commercial MgH_2 powder (AA) and MgH_2–VO_2(B) composite (V). Catalyzed system shows three maxima positioned at 642 K (HT), 456 K (IT) and 354 K (LT).

different courses for H_2 desorption. Several explanation for this decrease in desorption temperature can be adopted, from catalytic effect of the oxides to the role of the oxides as a lubricating agent for the formation of finer MgH_2 particles with a high density of interfaces [5,6,9,23–27]. Catalytic effect of vacancy-rich transition metal oxides could be explained in the line of following remarks: during mechanical milling a significant accumulation of highly reactive, low-coordinated surface centers were formed, which are related to two fundamentally different processes of H_2 chemisorption on oxides—the homolytic and the heterolytic dissociation of H_2 [28]. The homolytic process is initiated by the presence of $O^-$and M^+ radicals that gives rise to an irreversible formation of surface OH groups, while heterolytic dissociation of H_2 occurs in the course of a reversible process on the $M^{2+}$and O^{2-}ion pairs [28]. Further, according to Varin et al. [5] smaller particles provide larger surface area for H recombination, so the decrease of the mean particle as well as crystallite size of MgH_2–VO_2(B) composite has strong effect on hydrogen desorption temperature of MgH_2. As shown by Barkhordarian et al., one of the crucial factors for oxide to be an effective catalyst is high number of structural defects, such as vacancies [7]. In bulk, each transition-metal (TM) ion is surrounded by oxygen ions, but at the surface one oxygen ion is missing. This causes a change in the electronic structure of the metal ion, leading to the high catalytic activity of the oxide catalyst. Therefore, TM ions on the surface and in the bulk of oxides are under the influence of different crystal fields, which causes a splitting of the electronic 3d state in these ions and can be responsible for the catalytic behavior of transition-metal oxides in adsorption of gas molecules [29]. Borgschulte et al. proposed a pathway for hydrogen release through formation of oxide interfaces that are attached to the oxide catalyst that locally destabilize MgH_2. The number of these oxide interfaces, their stability and the amount of substoichiometric $MgH_{2-\delta}$, is determined by the type of catalyst and the preparation method [19,20]. Catalytic activity of transition-metal compounds can be explained by high number of structural defects, a low stability of the compound, high valence state of the transition-metal ion within the compound or high affinity of the transition-metal ion to hydrogen [7]. Among these factors, high number of structural defects is probably the most important factor regarding VO_2(B) oxides.

It is worth to notice that the temperature onset (T^d_{onset}) for all three desorption peaks are moved to lower values—HT maximum starts at 550 K, IT at 400 K, while LT maximum starts at 330 K. Therefore, the addition of small quantity of VO_2(B) as a catalyst has pronounced influence on the beginning of desorption process and also on the reaction mechanism.

The hydrogen desorption from metal hydrides consists of several different steps: physisorption, chemisorption (recombination), surface penetration, diffusion and hydride formation (decomposition). In general, the slowest step determines the kinetic rate [30]. The kinetic curve at each step has a characteristic form, which can be formulated as equation relating the transformed phase fraction to the time as it has been explained in experimental part. Therefore, it is possible to deduce the rate-limiting step of the kinetics, if a good fit of experimental data with a specific kinetic equation can be obtained. Several solid-state reaction mechanism models have been tested to select the best fitting form, including the nucleation-and-growth, the geometric contraction (R2 and R3), the diffusion, and the reaction order models based on the different geometry of the particles and the different driving forces as shown in Table 1 [31]. The obtained rate limiting steps of desorption reaction for composite material and pure MgH_2 are listed in Table 2 and Fig. 5. Regarding the composite material, the function based on phase boundary reaction with

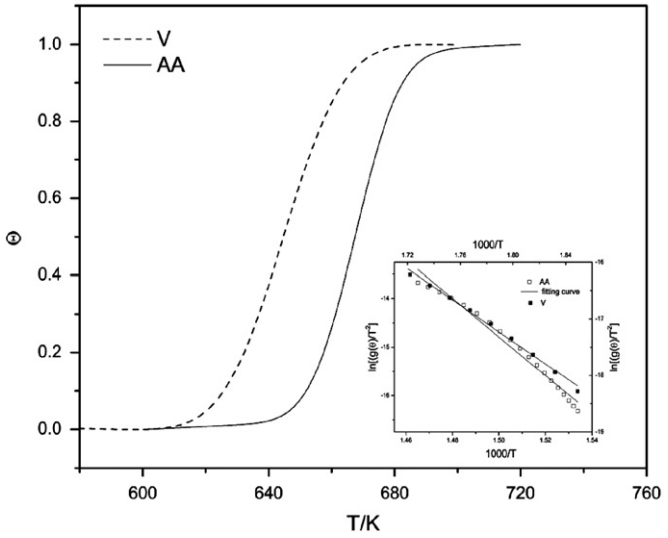

Fig. 5. Temperature evolution of the reacted fraction (θ) corresponding to MgH_2 decomposition, obtained by integration of HT-H_2 peak for commercial MgH_2 (AA), MgH_2–VO_2(B) composite (V) sample. Inserted figure: Form $\ln[g(\theta)/T^2] = f(1000/T)$ best fit of experimental data is obtained for geometric contraction (R2 and R3) (see Table 2).

Table 2
Rate limiting step for desorption reaction of pure MgH_2 (AA) and MgH_2–VO_2(B) composites (V).

Sample	Best linear fit	Mechanism
Commercial MgH_2	$\ln\left[\frac{1-(1-\theta)^{1\backslash 3}}{T^2}\right] = f\left(\frac{1000}{T}\right)$ $0.1 < \theta < 0.9$, $R^2 = 0.996$	Phase boundary reaction with spherical symmetry (R3)
MgH_2–VO_2(B)	$\ln\left[\frac{1-(1-\theta)^{1\backslash 2}}{T^2}\right] = f\left(\frac{1000}{T}\right)$ $0.1 < \theta < 0.9$, $R^2 = 0.994$	Phase boundary reaction with cylindrical symmetry (R2)

cylindrical symmetry gives the best results over the whole θ coverage range, while for untreated sample the best fit is obtained for phase boundary reaction with spherical symmetry (see insert in Fig. 5). Both used models belong to geometrical contraction (R) models that assume that nucleation occurs rapidly on the surface of the crystal. The rate of degradation is controlled by the resulting reaction interface progress towards the center of the crystal. Further, models depend on the shape of the crystals, so R2 (contracting area) model is based on cylindrical particles while R3 (contracting volume) model is based on spherical particles. From the slope of straight line (see Fig. 5 and Table 2), the activation energy of composite is estimated to be $E^a_{des} = 139(kJ/molH_2)$ which is reduced in comparison to the value obtained for non-treated MgH_2 ($E^a_{des} = 160(kJ/molH_2)$), meaning that VO_2 nanostructured oxide remarkably improves the kinetics of desorption process.

4. Conclusion

To investigate the catalytic activity of nanostructured VO_2 ceramics on hydrogen desorption and kinetics from MgH_2, ball milling of MgH_2 with monoclinic VO_2(B) have been performed. VO_2(B) was produced by one-step hydrothermal synthesis. Structural characterization of composite has been done by XRD, SEM and laser scattering particle size analysis. It has been shown that milling of MgH_2 with VO_2(B) induces changes in morphology and decrease of particles and crystallite size. DTA spectra of composite showed significant reduction of both, T^d_{onset} and T^d_{max}. This can be assigned to decrease in the particle size of pure MgH_2 and the catalytic activity of VO_2(B), mutually. The mechanism of desorption has been changed from phase boundary reaction with spherical symmetry to phase boundary reaction with cylindrical symmetry when vacancy-rich VO_2(B) oxide is added as catalyst.

Acknowledgment

This work is financially supported by the Serbian Ministry of Education and Science under grant III45012. Authors want to express their gratitude to Zvezdana Baščarević responsible for scanning electron microscopy and Zoran Stojanović responsible for particle size distribution measurements.

References

[1] L. Schlapbach, A. Züttel, Hydrogen-storage materials for mobile applications, Nature 414 (2001) 353–358.
[2] K.-F. Aguey-Zinsou, J.R. Ares Fernandez, T. Klassen, R. Bormann, Using MgO to improve the (de)hydriding properties of magnesium, Materials Research Bulletin 41 (6) (2006) 1118–1126.
[3] G. Barkhordarian, T. Klassen, R. Bormann, Kinetic investigation of the effect of milling time on the hydrogen sorption reaction of magnesium catalyzed with different Nb_2O_5 contents, Journal of Alloys and Compounds 407 (2006) 249–255.
[4] A. Montone, J. Grbović Novaković, M. Vittori Antisari, A. Bassetti, E. Bonetti, A.L. Fiorini, L. Pasquini, L. Mirenghi, P. Rotolo, Nano-micro MgH_2–Mg_2NiH_4 composites: tayloring a multichannel system with selected hydrogen sorption properties, International Journal of Hydrogen Energy 32 (14) (2007) 2926–2934.
[5] R.A. Varin, T. Czujko, Ch. Chiu, Z. Wronski, Particle size, grain size and γ-MgH_2 effects on the desorption properties of nanocrystalline commercial magnesium hydride processed by controlled mechanical milling, Nanotechnology 17 (15) (2006) 3856–3865.
[6] S. Kurko, Ž. Rašković, N. Novaković, B. Paskaš Mamula, Z. Jovanović, Z. Baščarević, J. Grbović Novaković, Lj. Matović, Hydrogen storage properties of MgH_2 mechanically milled with α and β SiC, International Journal of Hydrogen Energy 36 (1) (2011) 549–554.
[7] G. Barkhordarian, T. Klassen, R. Bormann, Catalytic mechanism of transition-metal compounds on Mg hydrogen sorption reaction, Journal of Physical Chemistry B 110 (22) (2006) 11020–11024.
[8] F. Tonus, V. Fuster, G. Urretavizcaya, F.J. Castro, J.-L. Bobet, Catalytic effect of monoclinic WO_3, hexagonal WO_3 and $H_{0.23}WO_3$ on the hydrogen sorption properties of Mg, International Journal of Hydrogen Energy 34 (2009) 3404–3409.
[9] A. Montone, J. Grbović, Lj. Stamenković, A.L. Fiorini, L. Pasquini, E. Bonetti, M. Vittori Antisari, Desorption behaviour in nanostructured MgH_2-Co, Materials Science Forum 518 (2006) 79–84.
[10] G. Liang, J. Huot, S. Boily, A. Van Neste, R. Schulz, Catalytic effect of transition metals on hydrogen sorption in nanocrystalline ball milled MgH_2-Tm (Tm=Ti, V, Mn, Fe and Ni) systems, Journal of Alloys and Compounds 292 (1999) 247–252.
[11] W. Oelerich, T. Klassen, R. Bormann, Metal oxides as catalysts for improved hydrogen sorption in nanocrystalline Mg-based materials, Journal of Alloys and Compounds 315 (1–2) (2001) 237–242.
[12] W. Oelerich, T. Klassen, R. Bormann, Comparison of the catalytic effects of V, V_2O_5, VN, and VC on the hydrogen sorption of nanocrystalline Mg, Journal of Alloys and Compounds 322 (1–2) (2001) L5–L9.
[13] W. Oelerich, T. Klassen, R. Bormann, Mg-based hydrogen storage materials with improved hydrogen sorption, Materials Transactions 42 (8) (2001) 1588–1592.
[14] W. Oelerich, T. Klassen, R. Bormann, Hydrogen sorption of nanocrystalline Mg at reduced temperatures by metal-oxide catalysts, Advanced Engineering Materials 3 (7) (2001) 487–490.
[15] M. Khrussanova, M. Terzieva, P. Peshev, On the hydriding of a mechanically alloyed Mg(90%)V_2O_5(10%) mixture, International Journal of Hydrogen Energy 15 (11) (1990) 799–805.
[16] K.S. Jung, E.Y. Lee, K.S. Lee, Catalytic effects of metal oxide on hydrogen absorption of magnesium metal hydride, Journal of Alloys and Compounds 421 (1–2) (2006) 179–184.
[17] I.E. Malka, J. Bystrzycki, T. Plocinski, T. Czujko, Microstructure and hydrogen storage capacity of magnesium hydride with zirconium and niobium fluoride additives after cyclic loading, Journal of Alloys and Compounds 509 (2) (2011) S616–S620.
[18] I.E. Malka, T. Czujko, J. Bystrzycki, Catalytic effect of halide additives ball milled with magnesium hydride, International Journal of Hydrogen Energy 35 (4) (2010) 1706–1712.
[19] A. Borgschulte, U. Bosenberg, G. Barkhordarian, M. Dornheim, R. Bormann, Enhanced hydrogen sorption kinetics of magnesium by destabilized $MgH_{2-\delta}$, Catalysis Today 120 (2007) 262–269.
[20] A. Borgschulte, M. Bielmann, A. Zuttel, G. Barkhordarian, M. Dornheim, R. Bormann, Hydrogen dissociation on oxide covered MgH_2 by catalytically active vacancies, Applied Surface Science 254 (2008) 2377–2384.
[21] S. Milošević, I. Stojković, S. Kurko, J. Grbović Novaković, N. Cvjeticanin, The simple one-step solvothermal synthesis of nanostructurated VO_2(B), Ceramics International 38 (3) (2012) 2313–2317.
[22] J. Sestak, G. Berggren, Study of the kinetics of the mechanism of solid-state reactions at increasing temperatures, Thermochimica Acta 3 (1) (1971) 1–12.

[23] Lj. Matović, N. Novaković, S. Kurko, M. Šiljegović, B. Matović, N. Romčević, N. Ivanović, J. Grbović Novaković, Structural destabilisation of MgH_2 obtained by heavy ion irradiation, International Journal of Hydrogen Energy 34 (17) (2009) 7275–7282.

[24] J. Grbović Novaković, Lj. Matović, M. Drvendžija, N. Novaković, D. Rajnović, M. Šiljegović, Z. Kačarević Popović, S. Milovanović, N. Ivanović, Changes of hydrogen storage properties of MgH_2 induced by heavy ion irradiation, International Journal of Hydrogen Energy 33 (7) (2008) 1876–1879.

[25] F. Leardini, J.R. Ares, J. Bodega, J.F. Fernandez, I.J. Ferrer, C. Sanchez, Reaction pathways for hydrogen desorption from magnesium hydride/hydroxide composites: bulk and interface effects, Physical Chemistry Chemical Physics 12 (3) (2010) 572–577.

[26] J.R. Ares, F. Leardini, P. Díaz-Chao, J. Bodega, J.F. Fernández, I.J. Ferrer, C. Sánchez, Ultrasonic irradiation as a tool to modify the H-desorption from hydrides: MgH_2 suspended in decane, Ultrasonics Sonochemistry 16 (2009) 810–816.

[27] A. Bassetti, E. Bonetti, L. Pasquini, A. Montone, J. Grbović, M. Vittori Antisari, Hydrogen desorption from ball milled MgH_2 catalyzed with Fe, European Physical Journal B 43 (2005) 19–37.

[28] E. Knozinger, K.-H. Jacob, P. Hofmann, Adsorption of hydrogen on highly dispersed MgO, Journal of the Chemical Society, Faraday Transactions 89 (7) (1993) 1101–1107.

[29] B. Fromme, d–d Excitations in Transition-Metal Oxides, A Spin-Polarized Electron Energy-Loss Spectroscopy (SPEELS) Study, Springer Tracts in Modern Physics, Springer, New York, 2001 (vol. 170).

[30] J. Gulicovski, Ž. Rašković-Lovre, S. Kurko, R. Vujasin, Z. Jovanović, Lj. Matović, J. Grbović Novaković, Influence of vacant CeO_2 nanostructured ceramics on MgH_2 hydrogen desorption properties, Ceramics International 38 (2) (2012) 1181–1186.

[31] R. Ebrahimi-Kahrizsangi, M.H. Abbasi, Evaluation of reliability of Coats–Redfern method for kinetic analysis of non-isothermal TGA, Transactions of Nonferous Metals Society of China 18 (1) (2008) 217–221.